15.2

THE VERTICAL STRUCTURE OF A TORNADO: HIGH-RESOLUTION, W-BAND, DOPPLER-RADAR OBSERVATIONS NEAR HAPPY, TEXAS ON 5 MAY 2002

Howard B. Bluestein* and Christopher C. Weiss
University of Oklahoma
Norman, Oklahoma

Andrew L. Pazmany+
University of Massachusetts
Amherst, Massachusetts

1. INTRODUCTION

The vertical and radial variation of wind speeds in tornadoes is of great interest to both theoreticians and structural engineers. From experiments with laboratory models (e.g., Church et al. 1979) and large-eddy simulation models of tornado-like vortices (e.g., Lewellen et al. 2000), it is known that the radial and vertical profiles of the vertical and horizontal wind depend upon the swirl ratio.

Until recently, radar measurements in real tornadoes, have been few. Wakimoto and Martner (1992), using two fixed-site X-band radars whose antennas had a 0.8° beamwidth, and Wurman and Gill (2000), using a mobile X-band Doppler radar whose antenna had a 1.2° beamwidth, produced vertical cross sections of Doppler velocity and radar reflectivity through a landspout in Colorado and a supercell tornado in West Texas, respectively, by synthesizing data collected in scans at constant elevation angle.

Resolving air motions as close to the ground as possible requires a very narrow beam and a relatively weak sidelobe pattern. To achieve even higher spatial resolution, a W-band (3-mm wavelength) truck-mounted pulsed Doppler radar system has been used to probe tornadoes in the southern Plains (Bluestein and Pazmany 2000). The antenna of this radar system has a half-power beamwidth of only 0.18°.

The main purpose of this paper is to describe the vertical variation of radar reflectivity and Doppler velocity in a tornado near Happy, TX on 5 May 2002. In addition, the analyses of the radar data will be correlated with visual features. A more detailed treatment of this case is found in (Bluestein et al. 2004b).

2. DATA COLLECTION AND PROCESSING

Data were collected beginning when the tornado, which was mature, was passing through and east of Happy, TX, located 7.2 km to the west-southwest of the radar. The tornado inflicted "extensive" damage (www.spc.noaa.gov/climo/) as it moved through the town at about 1945 CDT (all times given in CDT) and continued east-northeastward toward the radar. Several homes were destroyed and a roof was blown off a church; three people were killed and four were injured.

Low-elevation-angle sector scans (just above the ground) were collected first while the tornado was 6.2 – 4.4 km away. Then a series of RHIs on the right sight, left side, and through the center of the tornado were collected while the tornado was at 3.1 - 1.6 km range; at these ranges the azimuthal resolution was only 10 - 20 m.

Figure 1. Tornado to the west-southwest of the W-band radar seen in the foreground along with the first author, at approximately 1949 CDT, 5 May 2002, 7.2 km east of Happy, TX. Photograph © M. Kramar.

Finally, more low-elevation-angle sector scans were collected as the tornado reached 1.1 km in range while it was dissipating. It was fortunate that the RHIs were collected when the range was within 3.1 km: Prior to then, attenuation seriously limited the intensity of the backscatter from the tornado and after then the tornado was too close (within 1.5 km) to do PDPP processing (Pazmany et al. 1999) and achieve a maximum unambiguous Doppler velocity of ±79 m s^{-1}; when only conventional pulse-pair processing was usable, the maximum unambiguous Doppler velocity was only ±8 m s^{-1}, which made unfolding aliased data difficult, if not impossible.

The pulse length was set to 30 m, even though a pulse length of only 15 m was possible, because only 250 range gates could be stored; it was not possible to set the correct window to view the entire tornado quickly enough. So, the pulse volume when the RHIs were taken was about 15 m X 15 m X 30 m. However, data were collected every 15 m, so that the data were "oversampled." Each scan was accompanied by boresighted video so that the locations with respect to the visible condensation funnel and debris cloud could be determined. From the boresighted video, it was determined that the radar platform was tilted approximately 5° to the right, or toward the north.

As a result of a software malfunction, relative azimuth (in the constant elevation-angle sector scans) and elevation angles (in the RHIs) were not recorded.

---

* *Corresponding author address:* Howard B. Bluestein, School of Meteorology, Univ. of Oklahoma,Norman,OK 73019; e-mail: hblue@ou.edu
+Current affiliation: ProSensing, Inc., Amherst, MA

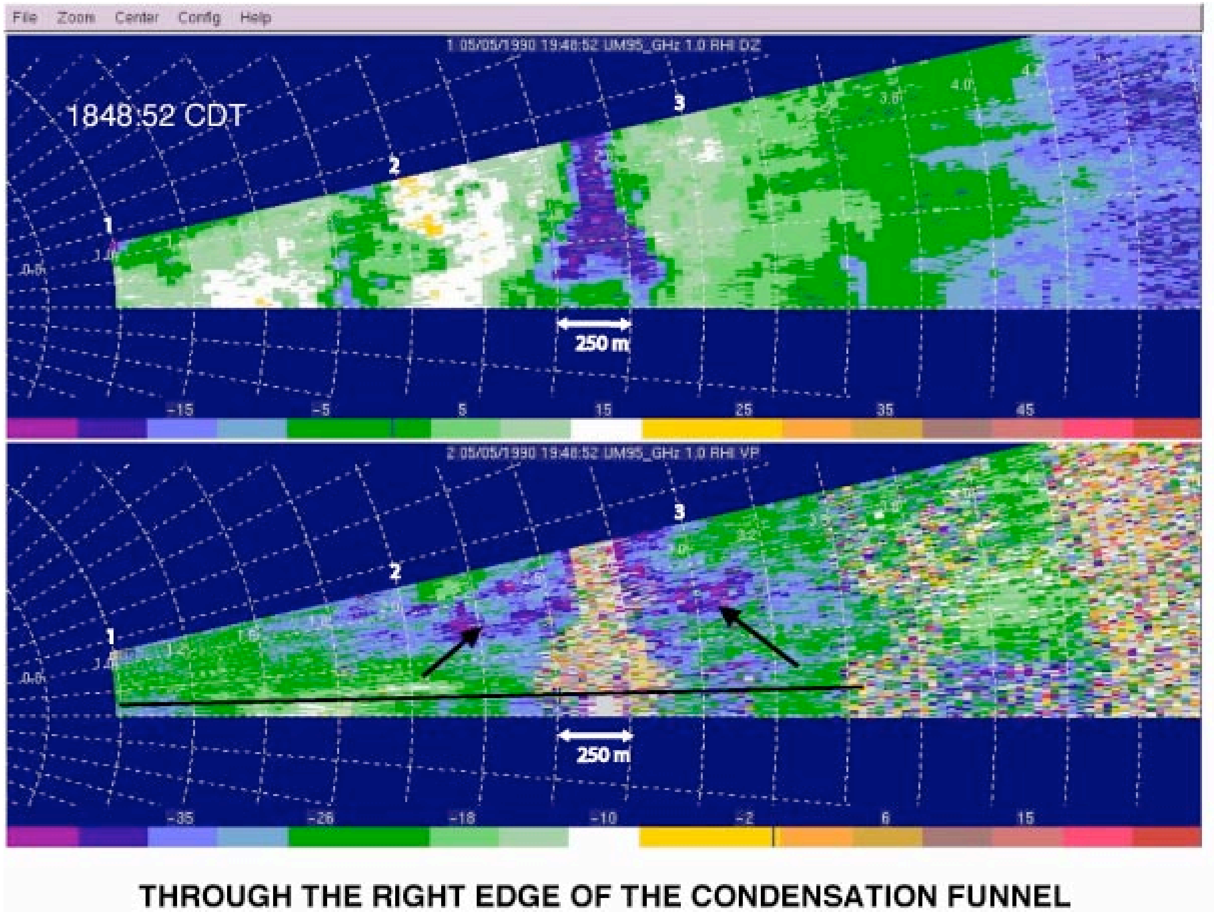

Figure 2. Vertical cross sections of radar reflectivity (dBZ) and ground-relative Doppler velocity (m s^{-1}) from the W-band radar (the radar is located to far left). The cross sections cut from the east-northeast (left-hand side) to the west-southwest (right-hand side), through the right edge of the tornado's condensation funnel. Color coded scales for reflectivity and Doppler velocity are shown below each panel. Positive (negative) Doppler velocities denote approaching (receding) motion. (There was a signal processing error that reversed the sign of the Doppler velocity. At 1848:52 CDT (time refers to the beginning of the scan, here and henceforth). Solid black line in the bottom, Doppler-velocity panel is the approximate horizon line. Arrows point to regions of high Doppler velocity away from the radar.

The azimuth and elevation angles were restored to the data record from each beam after viewing the boresighted video and from the known scan rates. Data collected while the antenna was not scanning and/or pointed at or below the ground level and/or at the top of each scan, were not included. It is therefore possible that some RHIs are shifted slightly when the ground is not exactly at 0° elevation angle.

The dimensions of the condensation funnel of the tornado and that of its surface debris cloud were determined by photogrammetrically analyzing medium-format (70 mm) transparencies taken by the first author. The distance to the visual features as a function of time was estimated from the radar data.

3. VERTICAL CROSS SECTIONS

The high-resolution RHIs are the unique aspect of the Happy, TX dataset. The center of the tornado was marked by a column of echo-weak/free hole. Above about 150 m AGL, the width of the hole was about 250 m (Figs. 2 – 4). The width of the hole was subjectively determined from the radar-reflectivity and Doppler-velocity fields. The width of the hole was the greatest for the scan that cut through the center of the tornado, as would be expected from geometrical considerations (Fig. 4).

The hole was pear shaped in general; it was approximately 40% wider at 100 m AGL than it was above. The width of the visible debris cloud was about 260 m, approximately the same as the width of the hole above 150 m AGL. The depth of the visible debris cloud was about 190 m. In a few of the vertical cross sections the echo hole closed up near the ground (Figs. 2 and 4).

Some of the echo holes tilt with height (e.g., Fig. 3). The tilts are artifacts related to the component of motion of the tornado toward the radar. When the radar antenna scanned upward, the echo hole tended to tilt

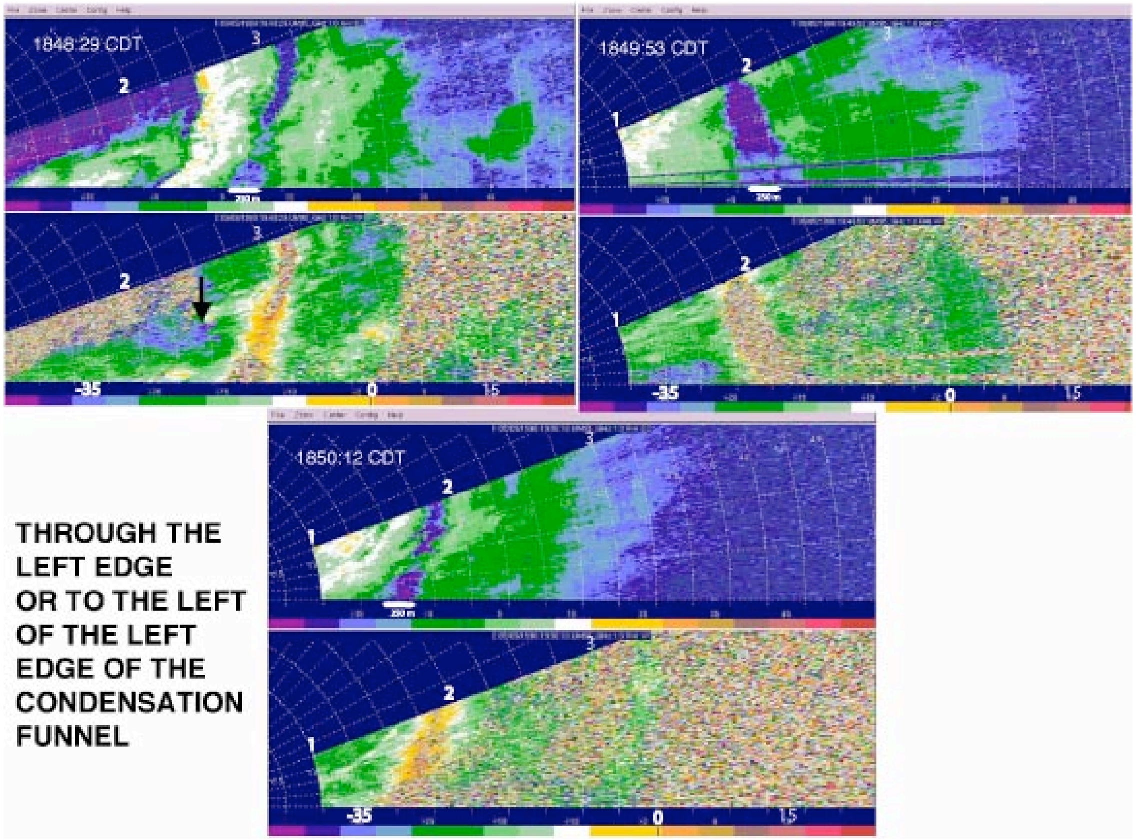

Figure 3. As in Fig. 2, but through the left edge or to the left of the left edge of the tornado's condensation funnel. At 1848:29 (upper left), 1849:53,(upper right), and 1850:12 CDT (bottom).

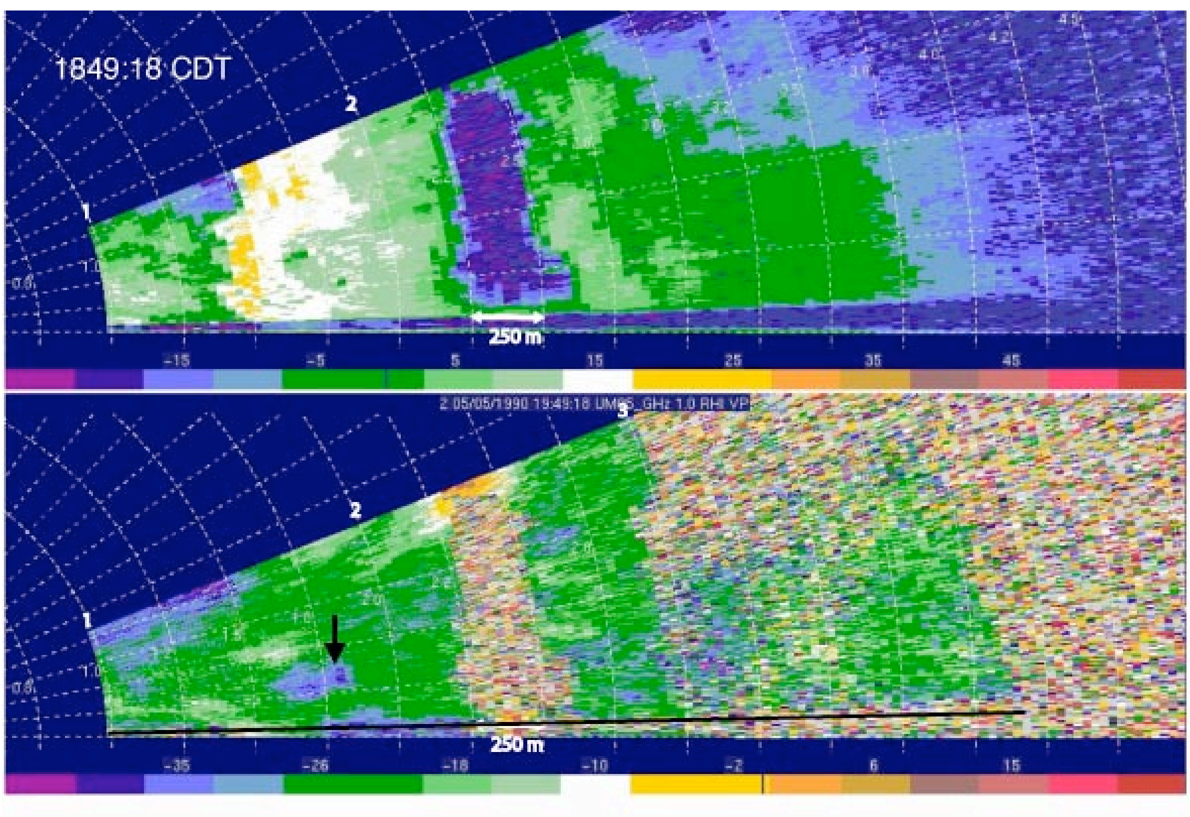

Figure 4. As in Fig. 2, but through the center of the tornado's condensation funnel. At 1849:18 CDT.

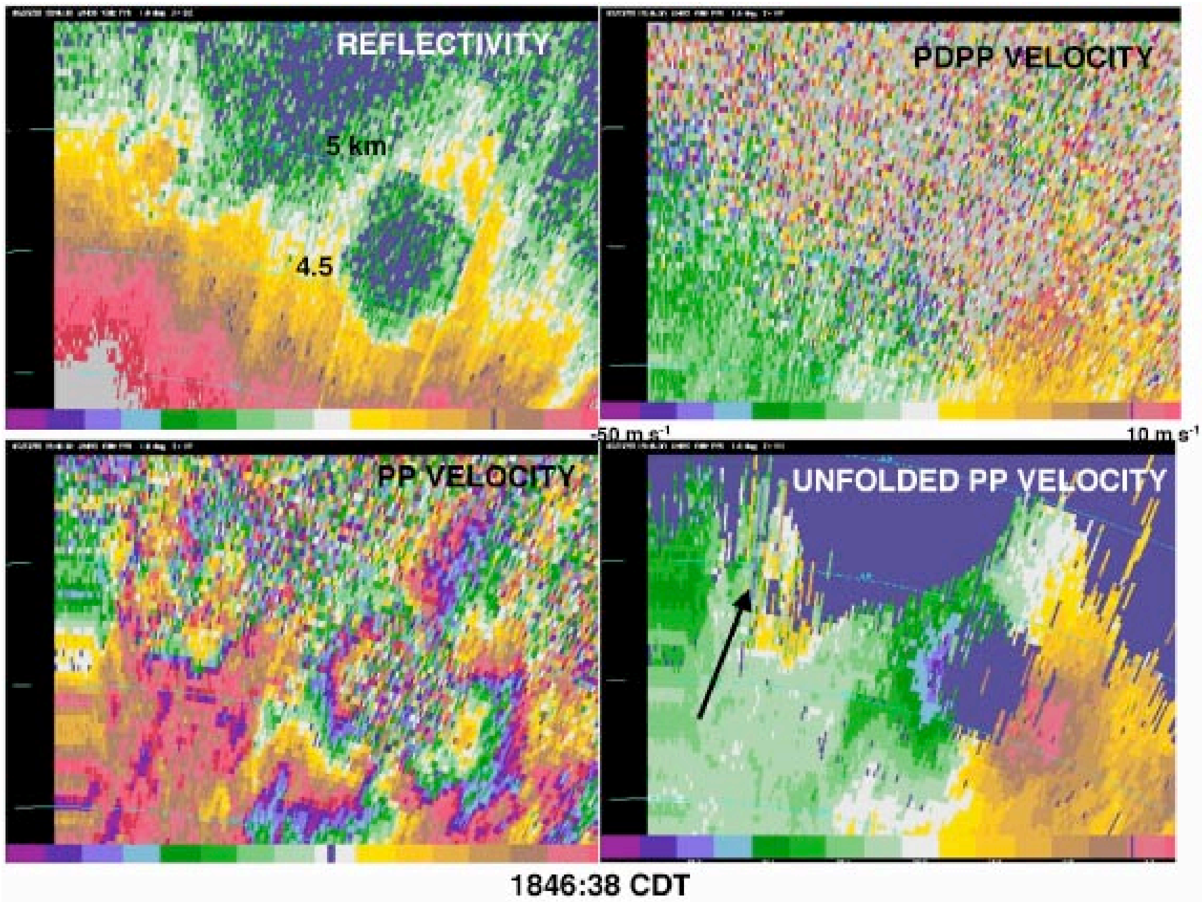

Figure 5. Portion of the sector scan at 1846:38 CDT. Range markings are shown every 500 m. In this figure only, positive (negative) Doppler velocities (m s^{-1}) denote motion away from (toward) the radar. Top left panel (radar reflectivity); top right panel (PDPP Doppler velocity); lower left panel (ordinary pulse-pair processed Doppler velocity; lower right panel (unfolded ordinary pulse-pair processed Doppler velocity). The arrow in the lower right panel points to a weak cyclonic vortex signature, to the left of the tornado. The tornado was located to the west-southwest of the radar.

toward the radar; when the radar antenna scanned downward, the hole tended to tilt away from the radar. From a series of PPI scans, it was determined that the component of motion of the tornado along the line-of-sight of the radar was about 13 m s^{-1}, toward the radar (i.e., from west-southwest to east-northeast). In the time it took the radar to complete an RHI scan (10 s or less), one extremity of the tornado had moved around 10 m closer than the opposite extremity.

To interpret the RHIs properly, it is necessary to relate the edges of the tornado's condensation funnel to the characteristics of the tornado vortex. From photogrammetric analysis, it was determined that the width of the condensation funnel at cloud base was approximately 70 m. So, the echo hole was wider than the condensation funnel. In Fig. 5 it is seen that the width of the core of the tornado was greater than the width of the condensation funnel. None of the RHIs exhibited very high Doppler velocities. It is therefore likely that none of the vertical cross sections cut across the core of the tornado, even though some were to the left/right of the condensation funnel.

In the vertical cross section cutting through the right edge of the tornado's condensation funnel (Fig. 2), there is an inflow jet about 200 – 400 m AGL, as strong as 35 – 40 m s^{-1}, cutting completely across the weak-echo hole.

In the vertical cross section cutting through the center of the tornado's condensation funnel, there was a region of low values of ground-relative Doppler velocity (white-yellow region) above and radially outward from an elevated jet (blue-purple region) (Fig. 4). This couplet in Doppler velocity might be indicative of a vertical circulation associated with frictional return flow or with a horizontal roll like that sometimes seen in LES simulations (e.g., Lewellen et al. 2000, their Fig. 5). Also, in Fig. 4, there is a region of enhanced inflow in the lowest few elevation scans about 500 m east of the center of the tornado. This inflow might be part of the actual surface inflow layer.

In the vertical cross sections cutting through the left part (closest to the radar, east-northeast) of the tornado

(Fig. 3) there is at 1848:29 CDT only, evidence of a wedge in reflectivity and an inflow jet near the wedge, and indications of outflow near the ground (yellow region). This pattern looks similar to what one would see along a gust front. Such a pattern was not evident in the next two scans taken to the left of the tornado (1849:53 and 1850:12 CDT), perhaps because that part of the tornado responsible for this pattern was within a kilometer of the radar, which was within the range window for which data were recorded.

3. SUMMARY AND CONCLUSIONS

The Happy, TX dataset was the first one in which we collected RHI data through a tornado with the W-band radar. The reflectivity structure is similar in a few respects to that found by Wurman and Gill (2000). In each, the hole does not extend all the way down to the ground; also, the diameters of the echo-free eyes are similar.

A different feature of the Happy, TX eye is its broadening out just above the ground; it is widest at 100 m AGL, the approximate height of the midlevel of the visible debris cloud. It is hypothesized that this broadening may be due to centrifuging of scatterers radially outward near or just within the tornado core or as a result of the secondary circulation of the tornado, in which there is radial outflow above the surface friction layer. The hole narrows below, perhaps owing to the inward transport of scatterers in the surface friction layer. Dowell et al. (2005) has numerically simulated tornadolike vortices having particles of various sizes injected into it. Such a study could explain more quantitatively the observed shape of the eye's reflectivity profile.

The height AGL at which the maximum azimuthal wind speeds in tornadoes is found varies with the swirl ratio and the nature of the boundary conditions (Lewellen et al. 2000). It was surprising that the highest wind speeds were found so high, around 300 m AGL (Golden and Purcell (1977). The result could have been different, however, if the core had actually been sampled. In addition, the effects of turbulence and the transient nature of the tornado vortex should be accounted for by sampling as often as possible.

The elevated inflow jet could be explained as follows: (a) evaporatively cooled air as part of a gust front could have wrapped around the tornado from its south side just before the tornado dissipated; inflow air could have been lifted over this cold pool of air as it flowed towards the tornado; Fig. 3 (upper-left panel) is consistent with this hypothesis; (b) the surface-boundary–layer jet was asymmetrically distributed around the tornado (Golden and Purcell 1977) and the viewing angle of the radar was normal to the jet; (c) the surface inflow layer was so shallow that it was below the radar horizon; (d) the elevated jet was a manifestation of a horizontal roll.

In the case of the Happy, TX tornado, the motion of the tornado had a significant component along the line-of-sight of the radar. It would be better for data collection if the tornado moved largely across the line of sight, so that RHIs could be taken at a fixed location; then, as the tornado translated by the plane scanned in the RHI, the spatial resolution across the tornado would be maximized, and its core could be sampled.

In addition, since the core of the tornado likely lies outside the visible edge of the condensation funnel (e.g., Bluestein et al. 2003), RHIs should begin well to the side of the condensation funnel. Furthermore, there is some evidence that debris clouds at the surface in intense vortices can be narrower than the core diameter (Bluestein et al. 2003; Bluestein et al. 2004). It is thus concluded that RHI scans should begin outside the edge of the debris cloud also and that the tornado should then pass through the RHI plane until the opposite edge of the debris cloud has passed. Efforts to minimize the effects of tilting of the RHI plane should be undertaken by more carefully leveling the radar platform.

Knowledge of the core diameter of the tornado being sampled is very important. If attenuation makes it difficult to determine the core diameter when using sector scans, then it may be necessary to increase the pulse length of the radar to enhance the sensitivity at the expense of along-the-line-of-sight spatial resolution.

On 12 May 2004, W-band radar data were collected in a tornado near Attica, Kansas. The tornado was just 2 – 3 km away and excellent visibility allowed for clear, boresighted video documentation while the antenna was scanning. Owing to range gates only 15 m long and the close range to the tornado, very high spatial resolution PPIs and RHIs were attained. If time permits, a preliminary look at an RHI from this dataset will be shown.

ACKNOWLEDGMENTS

This research was funded by NSF grants ATM-9912097 and ATM-0241037 at OU and ATM-9616730 at U. Mass. Support was also provided by the School of Meteorology at the University of Oklahoma (OU). The second author operated the radar in the field. Brendan Fennell also participated in this field project.

REFERENCES

Bluestein, H. B., C. C. Weiss, and A. L. Pazmany, 2004a: Doppler-radar observations of dust devils in Texas. *Mon. Wea. Rev.*, **132**, 209 – 224.

____________,____________,and_____________, 2004b: The vertical structure of a tornado near Happy, Texas, on 5 May 2002: High-resolution, mobile, W-band, Doppler radar observations. *Mon. Wea. Rev.*, **132**, (in press)

____________, W.-C. Lee, M. Bell, C. C. Weiss, and A. L. Pazmany, 2003: Mobile-Doppler-radar observations of a tornado in a supercell near Bassett, Nebraska on 5 June 1999. Part II: Tornado-vortex structure. *Mon. Wea. Rev.*, **131**, 2968 – 2984.

_____________, and A. L. Pazmany, 2000: Observations of tornadoes and other convective phenomena with a mobile, 3-mm wavelength, Doppler radar: The spring 1999 field experiment. *Bull. Amer. Meteor. Soc.*, **81**, 2939-2951.

Church, C. R., J. T. Snow, G. L. Baker, and E. M. Agee, 1979: Characteristics of tornado-like vortices as a function of swirl ratio: A laboratory investigation. *J. Atmos. Sci.*, **36**, 1755-1776.

Dowell, D. C., C. R. Alexander, J. M. Wurman, and L. J. Wicker, 2005: Centrifuging of hydrometeors and debris in tornadoes: Radar-reflectivity patterns and wind-measurement errors. *Mon. Wea. Rev.* (in review)

Golden, J. H., and D. Purcell, 1977: Photogrammetric velocities for the Great Bend, Kansas, tornado of 30 August 1974: Accelerations and asymmetries. *Mon. Wea. Rev.*, **105**, 485 – 492.

Lewellen, D. C., W. S. Lewellen, and J. Xia, 2000: The influence of a local swirl ratio on tornado intensification near the surface. *J. Atmos. Sci.*, **57**, 527-544.

Pazmany, A. L., J. C. Galloway, J. B. Mead, I. Popstefanija, R. E. McIntosh, and H. B. Bluestein, 1999: Polarization diversity pulse pair technique for millimeter-wave Doppler radar measurements of severe-storm features. *J. Atmos. Ocean. Tech.*, **16**, 1900-1911.

Wakimoto, R. M., and B. E. Martner, 1992: Observations of a Colorado tornado. Part II: Combined photogrammetric and Doppler radar analysis. *Mon. Wea. Rev.*, **120**, 522-543.

Wurman, J., and S. Gill, 2000: Finescale radar observations of the Dimmitt, Texas (2 June 1995), tornado. *Mon. Wea. Rev.*, **128**, 2135-2164.